

# M-body density functional theory and the generalized hypernetted-chain equation

Toyonori Munakata<sup>a)</sup> and Kang Kim

*Department of Applied Mathematics and Physics, Kyoto University, Kyoto 606, Japan*

(Received 12 October 1999; accepted 16 June 2000)

The HNC (hypernetted-chain) theory for two-body correlation in fluids is generalized so that up to  $M$ -body ( $M > 2$ ) correlation functions can be obtained self-consistently. Our approach is based on the  $M$ -body density functional theory and a generalized Percus idea where maximally  $M - 1$  particles are held fixed in space, leading to  $M - 1$  HNC equations for the correlation functions. These are supplemented with  $M - 1$  Ornstein-Zernike relations to give a closed set of equations. Due to the rather complicated structure of the coupled integral equations, we explicitly present the equations for the case  $M = 3$ , which are compared with the HNC2 equations by Verlet. The  $M = 3$  theory is numerically solved for the case of a one-dimensional liquid. © 2000 American Institute of Physics. [S0021-9606(00)51934-5]

## I. INTRODUCTION

The density functional theory (DFT) of nonuniform fluids has been playing an important role in classical many-body theory.<sup>1</sup> It has been successfully applied in quantitative studies on solid–liquid transformations, including interfacial and nucleation phenomena, and so on.<sup>2</sup> Recently the DFT has been extended in various ways, e.g., to investigate molecular systems<sup>3</sup> and dynamic aspects of various phenomena mentioned previously.<sup>4</sup>

It is remarked here that the DFT is closely related to the equilibrium theory for structure of uniform fluids.<sup>5</sup> That is, if one has a reliable expression or approximation for the free-energy density functional  $F[n(\mathbf{r})]$ , with  $n(\mathbf{r})$  denoting a density field for a fluid, one can derive a good equation for the radial distribution function  $g_2(r) = 1 + h_2(r)$  which represents two-body correlations in a fluid.

To illustrate this interconnection, we consider a simple  $d$ -dimensional liquid with interparticle interaction  $\phi(r)$ . First let us hold, following Percus,<sup>6</sup> a particle fixed at the origin of the coordinate system. Then the (equilibrium) density  $n(\mathbf{r})$ , which obeys the variational Eq. (1), just represents  $n_0 g_2(r)$  with  $n_0$  being the uniform density,

$$\delta F / \delta n(\mathbf{r}) + \phi(r) = \mu, \quad (1)$$

with  $\mu$  a chemical potential. The two-body approximation for  $F[n(\mathbf{r})]$  is given by<sup>1,2</sup>

$$\begin{aligned} F_2[n] &= k_B T \int d\mathbf{r} n(\mathbf{r}) \ln[n(\mathbf{r}) \Lambda^d] \\ &\quad - (k_B T/2) \int d\mathbf{r} \int d\mathbf{r}' \delta n(\mathbf{r}) c_2(|\mathbf{r} - \mathbf{r}'|) \delta n(\mathbf{r}') \\ &\equiv F_{\text{id}} + F_{\text{ex}}^{(2)}, \end{aligned} \quad (2)$$

where  $\Lambda$  is the thermal wavelength and  $\delta n(\mathbf{r}) \equiv n(\mathbf{r}) - n_0$ .  $F_{\text{id}}$  and  $F_{\text{ex}}^{(2)}$  denote the ideal gas part and the two-body con-

tribution to the excess part, respectively. The two-body direct correlation function  $c_2(r)$  multiplied by  $-k_B T$  is seen to represent an effective interaction. The  $c_2(r)$  is related to the two-body total correlation function  $h_2(r) \equiv g_2(r) - 1$  via an exact two-body Ornstein-Zernike equation,<sup>5</sup>

$$\begin{aligned} h_2(r) &= c_2(r) + n_0 \int d\mathbf{r} h_2(|\mathbf{r} - \mathbf{r}'|) c_2(r') \\ &\equiv c_2(r) + n_0 h_2 * c_2(r). \end{aligned} \quad (3)$$

Inserting Eq. (2) into the variational equation (1) and taking into account the fact that  $n(\mathbf{r}) = n_0 g_2(r)$  is normalized to  $n_0$  at infinity or  $g_2(r \rightarrow \infty) = 1$ , we immediately obtain the (two-body) hypernetted-chain (HNC) equation

$$\ln g_2(r) = -[\phi(r) - n_0 k_B T h_2 * c_2(r)] / (k_B T). \quad (4)$$

Thus we have two equations, (3) and (4), for the two unknowns  $c_2(r)$  and  $g_2(r)$ . The terms in the square brackets on the right-hand side of Eq. (4) express the potential field felt by a particle at  $\mathbf{r}$ . The first term represents the direct field produced by a particle put at the origin and the second the indirect one produced by the surrounding particles.

The HNC equation has been applied to many kinds of fluids to study their structures and turned out to be very useful for theoretical prediction of  $g_2(r)$  up to the density slightly lower than that at the freezing point.<sup>5</sup> It is noted in passing that the HNC theory was first derived not based on the DFT theory but on some mathematical or diagrammatical argument.<sup>5,7</sup> However, the physical and concise DFT approach just presented suggests that we can rather straightforwardly extend the two-body HNC theory to higher order ones and this is what we try to do in this paper.

In Sec. II we develop a general  $M$ -body HNC theory based on the DFT. In Sec. III we investigate the case  $M = 3$  by explicitly writing down the closed set of equations for two- and three-body correlation functions. This is first compared with another extension of the HNC theory, i.e., the HNC2 by Verlet,<sup>8</sup> and the virial coefficients are discussed. The  $M = 3$  theory is then solved numerically for a one-

<sup>a)</sup>Electronic mail: munakatauamp.kyoto-u.ac.jp

dimensional liquid and some preliminary results for two- and three-body correlations are presented. Finally in Sec. IV we conclude the paper with some remarks.

## II. M-BODY HNC THEORY

Let us generalize the argument to derive the HNC equation (4) and establish a theory to deal with (up to)  $M$ -body ( $M > 2$ ) correlation functions self-consistently. For this purpose we approximate  $F_{\text{ex}}$  by including up to the  $M$ -th order terms as

$$F_{\text{ex}}[n] \approx \sum_2^M F_{\text{ex}}^{(j)}[n], \quad (5)$$

where  $F_{\text{ex}}^{(j)}[n]$  contains the  $j$ th order direct correlation function  $c_j(1,2,\dots,j)$  with 1 denoting  $\mathbf{r}_1$ . Thus explicitly we have, e.g.,

$$\begin{aligned} F_{\text{ex}}^{(j)}[n] = & -(k_B T / j!) \int d1 \cdots \int dj c_j(1,2,\dots,j) \\ & \times \delta n(1) \cdots \delta n(j). \end{aligned} \quad (6)$$

The first step of our  $M$ -body HNC theory is to notice that for the  $M$ -body correlation function  $g_M(1,\dots,M)$ , which is normalized to unity at infinity, we have

$$\begin{aligned} g_M(1,\dots,M) &= g_{M-1}(1,\dots,M-1)g_1(M|1,\dots,M-1) \\ &= g_1(2|1)g_1(3|1,2)g_1(4|1,2,3)\cdots \\ &\quad g_1(M|1,2,\dots,M-1), \end{aligned} \quad (7)$$

where, for example,  $n_0 g_1(4|1,2,3)$  represents a one-body distribution function at 4 when three particles are located at 1, 2, and 3. If  $M$  points  $\{1,2,\dots,M\}$  are regarded as points on a time axis, Eq. (7) reminds us of a non-Markovian stochastic process.<sup>9</sup> Furthermore this non-Markovian property is similar in its origin to that in the random-walk interpretation of polymer conformation (the excluded volume effect).<sup>10</sup>

Assuming that  $c_j(1,\dots,j)$  ( $j=2,\dots,M$ ) are known, we follow the idea of Percus<sup>6</sup> (this time however, maximally  $M-1$  particles are held fixed in space) to derive an equation for  $\ln g_1(j|1,2,\dots,j-1)$  ( $j=2,\dots,M$ ), based on Eqs. (1), (5), and (6) and the fact that the external field appearing on the left-hand side of the variational equation (1) is the sum of the field produced by particles located at 1, 2,..., and  $j-1$ . From this we readily obtain

$$\begin{aligned} \ln g_1(j|1,2,\dots,j-1) = & -\sum_{i=1}^{j-1} \phi(i,j)/(k_B T) \\ & + \Gamma_j^M [g_1(j|1,2,\dots,j-1) - 1], \end{aligned} \quad (8)$$

$$\begin{aligned} \Gamma_j^M[f] \equiv & \sum_{i=2}^M [n_0^{i-1}/(i-1)!] \int d1' \cdots \int d(i-1)' \\ & \times c_i(1',2',\dots,(i-1)',j)f(1') \cdots f((i-1)'), \end{aligned} \quad (9)$$

where  $f(1') \equiv g_1(1'|1,2,\dots,j-1) - 1$ . Thus we have  $M-1$  equations, Eq. (8) ( $j=2,\dots,M$ ) for  $M-1$  unknowns  $g_1(j|1,2,\dots,j-1)$  ( $j=2,\dots,M$ ).

As to the direct correlation functions, which were assumed to be known previously, we know that they are in a sense inverse functions of the correlation functions<sup>2,3,5</sup> and  $c_j(1,2,\dots,j)$  can be expressed in terms of  $g_k(1,2,\dots,k)$  ( $k=2,3,\dots,j$ ). This relation may be called the  $j$ -body Ornstein-Zernike relation. Thus in principle we have  $M-1$  relations between  $c_j(1,\dots,j)$  ( $j=2,\dots,M$ ) and  $g_j(1,\dots,j)$  ( $j=2,\dots,M$ ) and these complete the  $M$ -body HNC theory.

## III. THREE-BODY HNC THEORY

### A. Structure of three-body HNC equation

For concreteness and later convenience we write down explicitly the set of equations to determine  $g_2(1,2)$  and  $g_3(1,2,3)$  for the case  $M=3$ . First, Eq. (7) takes the form

$$g_3(1,2,3) = g_1(2|1)g_1(3|1,2), \quad (10)$$

where  $g_1(2|1)$  is nothing but the two-body radial distribution function  $g_2(1,2)$ . The HNC Eq. (8) for  $M=3$  is

$$\begin{aligned} \ln g_1(2|1) = & -\phi(1,2)/(k_B T) + n_0 \int d1' c_2(1',2) h_1(1'|1) \\ & + (n_0^2/2) \\ & \times \int d1' d2' c_3(1',2',3) h_1(1'|1) h(2'|1) \\ = & -\phi(1,2)/(k_B T) + C^{(2)} + B^{(2)}, \end{aligned} \quad (11)$$

$$\begin{aligned} \ln g_1(3|1,2) = & -(k_B T)^{-1} (\phi(2,3) + \phi(1,3)) \\ & + n_0 \int d1' c_2(1',3) h_1(1'|1,2) + (n_0^2/2) \\ & \times \int d1' \int d2' c(1',2',3) \\ & \times h_1(1'|1,2) h_1(2'|1,2) \\ = & -(k_B T)^{-1} (\phi(2,3) + \phi(1,3)) + C^{(3)} + B^{(3)}, \end{aligned} \quad (12)$$

where  $h_1(2|1) \equiv g_1(2|1) - 1$  and  $h_1(1|2,3) \equiv g_1(1|2,3) - 1$ . Comparing Eq. (11) with Eq. (4), we see that we have an extra contribution  $B^{(2)}$ , representing the potential field at 2 produced by particles at 1' and 2' through the (effective) three-body interaction  $c_3$ . This corresponds to the bridge function, which is neglected in the usual (two-body) HNC approximation.<sup>5</sup>

We now turn to the functions  $c_2$  and  $c_3$ , which are related to  $g_2$  and  $g_3$  through the Ornstein-Zernike (OZ) relations. The two- and three-body Ornstein-Zernike relations are most concisely expressed in terms of Fourier transformation as

$$\hat{h}_2(q) = \hat{c}_2(q)(1 + n_0 \hat{h}_2(q)), \quad (13)$$

$$\hat{H}(\mathbf{q}_1, \mathbf{q}_2) = \hat{c}_3(\mathbf{q}_1, \mathbf{q}_2) G(\mathbf{q}_1, \mathbf{q}_2), \quad (14)$$

where  $G(\mathbf{q}_1, \mathbf{q}_2) \equiv (1 + n_0 \hat{h}_2(q_1))(1 + n_0 \hat{h}_2(q_2))(1 + n_0 \hat{h}_2 \times (|\mathbf{q}_1 + \mathbf{q}_2|))$  and  $\hat{c}_3(\mathbf{q}_1, \mathbf{q}_2)$  denotes the Fourier transform of  $c_3(1,2,3)$  with 3 taken to be the origin of the coordinate system. Similarly  $\hat{H}(\mathbf{q}_1, \mathbf{q}_2)$  in Eq. (14) is defined as the Fourier transform of

$$\begin{aligned} H(1,2,3) &\equiv h_3(1,2,3) - h_2(1,2) - h_2(2,3) - h_2(1,3) \\ &- n_0 \int d4 h_2(1,4) h_2(2,4) h_2(3,4) \\ &- [h_2(1,2) h_2(2,3) + h_2(1,3) h_2(3,2) \\ &+ h_2(2,1) h_2(1,3)], \end{aligned} \quad (15)$$

with  $h_3(1,2,3) \equiv g_3(1,2,3) - 1$ . In summary we have now four integral equations—(11), (12), (14), and (15)—for four unknowns  $c_2, c_3, g_2$ , and  $g_3$  or  $g(3|1,2)$  supplemented by Eq. (10).

Before proceeding to numerical analysis of the case  $M=3$ , we briefly comment on the HNC2 equation<sup>8</sup> by Verlet, who extended the (functional) expansion method due to Percus<sup>6</sup> to explicitly include effects of three-body correlations. The HNC2 equation consists of Eq. (11) for the two-body correlation function and Eq. (12) without the  $B^{(3)}$  term for the three-body correlation function. As to the virial coefficients  $\{V_n\}$ <sup>5</sup> it gives the exact result up to fourth order (HNC is exact up to third order) and  $V_5$  for the hard sphere system from the HNC2 is 0.122 although the exact one is 0.11 and the superposition approximation (SA) gives 0.16.<sup>8</sup> Later we comment on the SA from the viewpoint of the  $M=3$  HNC theory. The contribution of  $B^{(3)}$  in Eq. (12) to the virial coefficients appears first at  $V_6$ , so our  $M=3$  theory and HNC2 give identical results as to  $V_5$ .

## B. Numerical study of the $M=3$ HNC theory

Looking at Eqs. (11) and (12) we immediately notice that Eq. (12) has a similar structure to that of Eq. (11). The difference comes from the fact that for Eq. (12) two particles are held fixed at 1 and 2, thus yielding two  $\phi$  terms and  $h_1$  function depending on two variables—1 and 2—in contrast to one  $\phi$  term and one variable 1 for Eq. (11). Setting the variable 1 in Eqs. (11) and (12) equal to the zero vector (the origin of the coordinate), we still have one variable “2” for Eq. (12), which is regarded as a parameter of Eq. (12). That is, Eq. (12) has to be solved for each value of the variable 2. In view of the similarity in structure of the HNC equations (11) and (12) with the two-body HNC equation (4), we employ the following procedure to solve the  $M=3$  theory: Starting from a trial (as to the first step, the ideal gas) direct correlation functions  $c_m^{\text{tr}}$  ( $m=2,3$ ), we calculate new ones  $c_m^{\text{new}}$  ( $m=2,3$ ). Then the new trial functions are taken to be a linear combination as

$$c_m^{\text{tr,new}} = (1 - w_m^{\text{new}}) c_m^{\text{tr}} + w_m^{\text{new}} c_m^{\text{new}} \quad (m=2,3), \quad (16)$$

with  $w_m^{\text{new}}$  ( $m=2,3$ ) denoting the weight for the new ones.<sup>5</sup> This constitutes one iteration, which consists of three steps. First, we calculate  $h_1$  functions on the right-hand side of Eqs. (11) and (12) based on the OZ equations (13) and (14) from  $c_2^{\text{tr}}$  and  $c_3^{\text{tr}}$ . Second, we make use of the HNC equations (11) and (12) to have new  $h_1$  functions. Finally, we calculate  $c_2^{\text{new}}$  and  $c_3^{\text{new}}$  functions from the new  $h_1$  functions, which is the opposite of the first step, and use Eq. (16) for new trial functions.

Numerical calculation was performed for a one-dimensional soft-rod system with  $\phi(r) = \epsilon(\sigma/r)^{12}$ .<sup>12</sup> A thermodynamic state of the system is characterized by one variable, which we take to be the nondimensional temperature  $T^* \equiv (k_B T / \epsilon)(l/\sigma)^{12}$  with  $l \equiv 1/n_0$ . One iteration mentioned previously took more than 10 min for our workstation but if we neglect the  $B^{(3)}$  term in Eq. (12), that is for HNC2, it took about 5 min or less for one iteration. For a one-dimensional system the two-body correlation function  $h_2(x) = g_2(x) - 1$  shows strong oscillatory behavior at low (high) temperature (density). In this case the correlation becomes long-ranged and the memory required for numerical calculations becomes large. One reason for our studying a one-dimensional system is the memory conservation and we consider the case  $T^* = 5000$  only, where  $h_2(x)$  is moderately oscillatory.

Here it is worthwhile to comment briefly on the convergence of iterative calculations. In the iteration step convergence is judged based on how the norm  $N_m \equiv \|c_m^{\text{new}} - c_m^{\text{tr}}\|$  ( $m=2,3$ ) changes as an iteration number increases. For HNC2 a weight  $w_m^{\text{new}} = 0.5$  ( $m=2,3$ ) in Eq. (16) worked well to attain convergence and we obtained rather oscillatory  $h_2(x)$  (several peaks are discernible), which corresponds to the structure with lower  $T^*$ . For  $M=3$  HNC, this weight does not work and we chose tentatively  $w_m^{\text{new}} = 0.1$  ( $m=2,3$ ) and the numerical results shown in the following are obtained at about 100 iterations. (After this the norm  $N_3$  began to increase slowly.) In this connection we note that fine tuning, which uses different values for  $w_2^{\text{new}}$  and  $w_3^{\text{new}}$ , may be necessary and this is left for future study.

In Fig. 1 we compare  $h_2(x)$  from numerical experiments ( $x > 0$ , a solid curve) and  $M=3$  ( $x < 0$ , a solid curve) theory with that from the usual ( $M=2$ ) HNC theory (a dotted curve). As is well known<sup>5</sup> and observed in Fig. 1, the  $M=2$  theory predicts a higher first peak and a more compressed structure compared with the experimental one. Our numerical solution to  $M=3$  HNC equations is seen to be similar to the  $M=2$  HNC results, with minor improvement in peak heights and positions. In Fig. 2 the  $C^{(2)}(x)$  (a solid curve) and  $10 \times B^{(2)}(x)$  (a dotted curve) are plotted. Although  $B^{(2)}$  is considerably smaller than  $C^{(2)}$  at this temperature, its effect on the phase relation (i.e., peak and valley positions) is seen to be in the right direction.

One advantage of the  $M=3$  theory is that various three-body correlations are obtained self-consistently. We depict in Fig. 3(a)  $C^{(3)}(x|y,z)$  (a dotted curve) and  $C_{SA}^{(3)}(x|y,z) \equiv C^{(2)}(xy) + C^{(2)}(xz)$  (a solid curve) and in Fig. 3(b)  $B^{(3)}(x|y,z)$  (a dotted curve) and  $B_{SA}^{(3)}(x|y,z) \equiv B^{(2)}(xy) + B^{(2)}(xz)$  (a solid curve) for  $y/l = 0.98$  and  $z/l = 0.0$ . If one employs the superposition approximation  $g_1(3|1,2)$

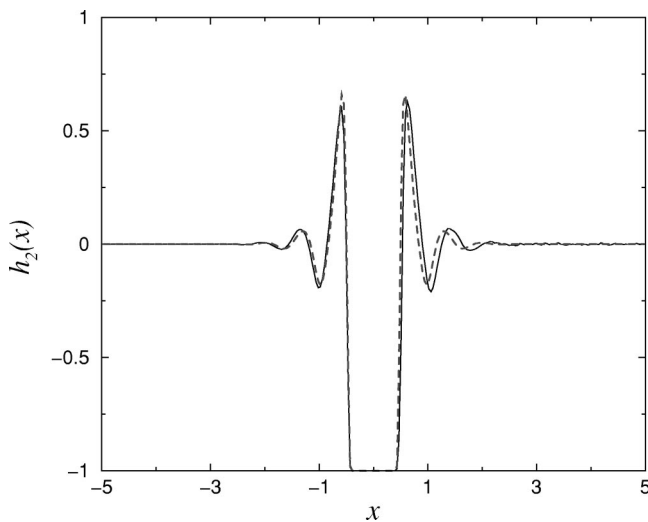


FIG. 1. The two-body correlation function  $h_2(x)$  from the two-body HNC theory (a dashed curve) is compared with the experiments ( $x > 0$ , a solid curve) and  $M=3$  HNC theory ( $x < 0$ , a solid curve).  $x$  is in units of the average interparticle length  $l = 1/n_0$  with  $n_0$  denoting the density for the one-dimensional system. In all the other figures the interparticle distance is measured this way.

$= g_1(3|1)g_1(3|2)$ , we see from Eqs. (11) and (12) that

$$C^{(3)}(x|y,z) = C_{SA}^{(3)}(x|y,z), \quad (17)$$

and a similar equation holds for  $B^{(3)}$ . We have confirmed numerically that in case three coordinates  $x$ ,  $y$ , and  $z$  are not clustered, the above-mentioned relation is satisfied. From Fig. 3 we notice considerable deviation from Eq. (17) when  $x$ ,  $y$ , and  $z$  are close to each other forming a cluster.

Summarizing this section, we tried to numerically solve the  $M=3$  theory and have shown some results for two- and three-body correlations. In view of the fact that even the HNC2 theory has not been numerically solved heretofore and that our scheme of calculations for  $M=3$  theory is not

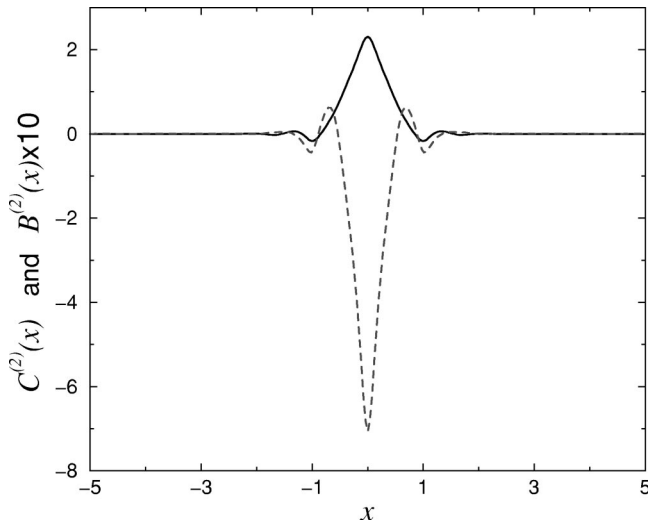


FIG. 2. The  $C^{(2)}(x)$  (a solid curve) and  $B^{(2)}(x)$  (a dashed curve) from  $M=3$  theory. Note that  $B^{(2)}(x)$  is multiplied by 10.

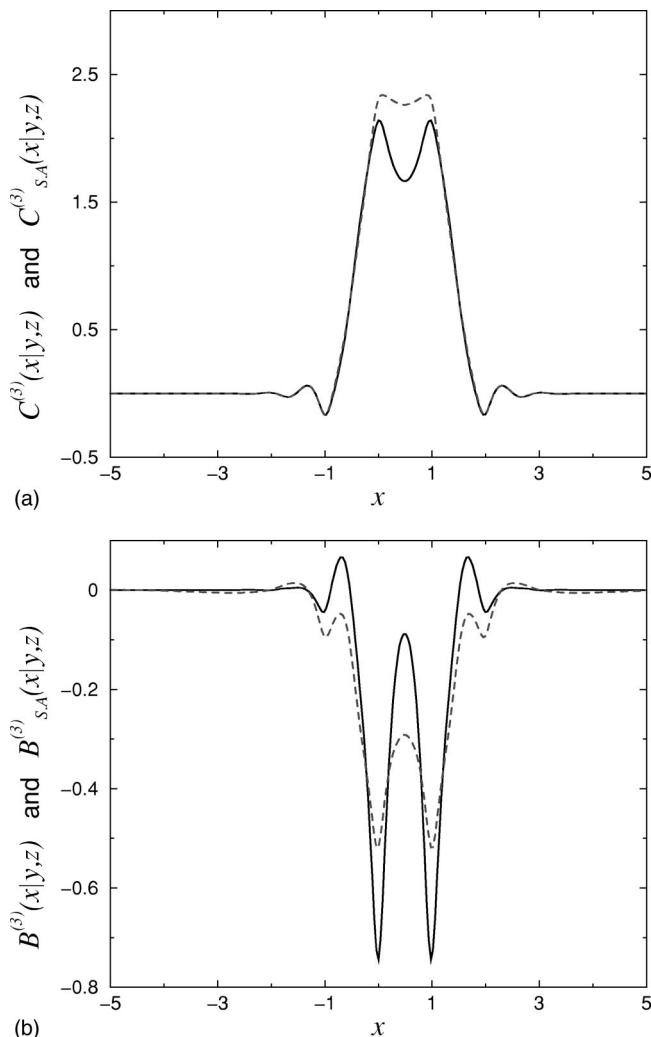


FIG. 3. (a)  $C^{(3)}(x|y,z)$  (a dashed curve) from the  $M=3$  HNC theory and the superposition approximation  $C_{SA}^{(3)}(x|y,z)$  (a solid curve) for  $y/l=0.98$  and  $z/l=0$ . (b)  $B^{(3)}(x|y,z)$  (a dashed curve) from the  $M=3$  HNC theory and the superposition approximation  $B_{SA}^{(3)}(x|y,z)$  (a solid curve) for  $y/l=0.98$  and  $z/l=0$ .

conclusive from the standpoint of convergence, we hope this topic will gather attention and more will be done for numerical as well as analytic investigation.

#### IV. SOME REMARKS

In this paper we developed a theory, which may be called an  $M$ -body HNC theory, to study structure of fluids systematically. This is based on the DFT and the non-Markovian expression (7) for higher-order correlation functions. As a first step in this direction we solved the self-consistent equations for the case  $M=3$  and compared the results for  $h_2(x)$  with experiments and the  $M=2$  HNC theory.

The usual ( $M=2$ ) HNC theory consists in neglecting the bridge function  $B^{(2)}$  in Eq. (11) entirely. To improve this, a bridge function of a suitable reference system was taken under the assumption that the bridge function has common features shared by simple fluids in general (a RHNC theory<sup>11</sup>). Based on the three-body DFT [ $M=3$  in Eq. (9)], a

more systematic approximation Eq. (11) was presented by Percus<sup>6</sup> and also by Verlet.<sup>8</sup> As far as we know, however, Eq. (12), which supplements Eq. (11) and two Ornstein-Zernike relations (13), (14), to give a closed set of equations for  $g_2(1,2)$  and  $g_3(1,2,3)$ , has not been given up to now. In passing it is noted that our theory is not limited to  $M=3$ . As  $M$  becomes large however, numerical solutions for the  $M$ -body HNC theory seem to be more and more difficult and it is highly desirable to have some general insights into the solution of the  $M$ -body ( $M=2,3,\dots$ ) HNC theory. This is seen also from the important roles played by the HNC theory to study static structures in liquids<sup>5</sup> and the glass transition.<sup>12</sup>

## ACKNOWLEDGMENTS

The author expresses his sincere gratitude to Professor F. Hirata (Institute for Molecular Science, Okazaki) and Professor M. Kinoshita (Kyoto University) for useful discussions and comments. He also thanks J. Yoshiwara (Hitachi Corpo-

ration) for help in numerical calculations at an early stage of this study.

<sup>1</sup>For reviews, see A. D. J. Haymet Annu. Rev. Phys. Chem. **38**, 89 (1987); D. W. Oxtoby, in *Liquid, Freezing, and the Glass Transition*, edited by J. P. Hansen, D. Levesque, and J. Zinn-Justin (Elsevier, New York, 1990).

<sup>2</sup>Y. Singh Phys. Rep. **207**, 351 (1991).

<sup>3</sup>D. Chandler, J. D. McCoy, and S. J. Singer, J. Chem. Phys. **85**, 5971 (1986) T. Munakata, S. Yoshida, and F. Hirata, Phys. Rev. E **54**, 3687 (1996).

<sup>4</sup>T. Munakata, Phys. Rev. E **50**, 2347 (1994); T. Takahashi and T. Munakata, *ibid.* **56**, 4344 (1997).

<sup>5</sup>J. P. Hansen and I. R. McDonald, *Theory of Simple Liquids* (Academic, New York, 1986).

<sup>6</sup>J. Percus, in *The Equilibrium Theory of Classical Fluids*, edited by H. L. Frisch and J. L. Lebowitz (Benjamin, New York, 1964).

<sup>7</sup>J. M. J. van Leeuwen, J. Groeneveld, and J. de Boer, Physica (Amsterdam) **25**, 792 (1959); T. Morita and H. Hiroike, Prog. Theor. Phys. **23**, 1003 (1960).

<sup>8</sup>L. Verlet, Physica (Amsterdam) **30**, 95 (1964); **31**, 959 (1965).

<sup>9</sup>C. W. Gardiner, *Handbook of Stochastic Methods* (Springer, Berlin, 1982).

<sup>10</sup>P. J. Flory, *Statistical Mechanics of Chain Molecules* (Interscience, New York, 1969).

<sup>11</sup>F. Lado, Phys. Rev. A **8**, 2548 (1973).

<sup>12</sup>M. Cardenas, S. Franz, and G. Parisi, J. Phys. A **31**, 163 (1998).